Mass Spectrometric Measurement Of the Ionization Energies and Cross Sections Of Uranium and Plutonium Oxide Vapors

F. Capone, Y. Colle, J. P. Hiernaut, and C. Ronchi*

European Commission, Joint Research Centre, European Institute for Transuranium Elements, Karlsruhe, Germany

Received: July 15, 1999; In Final Form: September 27, 1999

The ionization and dissociation energies of the different uranium and plutonium oxides have been measured by mass spectrometry of molecular beams produced by Knudsen effusion at high temperature. The values obtained constitute a set of self-consistent quantities, which are in agreement with the existing thermodynamic data of these oxides. On the basis of the experimental molecular parameters, general formulas for the ionization and dissociation/ionization cross sections due to electron inelastic scattering have been obtained for collision energies up to about 60 eV. These formulas are sufficiently accurate to calculate the composition of equilibrium vapor mixtures over UO_2 and PuO_2 from conventional mass spectrometric measurements.

I. Introduction

At high temperatures, the nonstoichiometric dioxides of uranium and plutonium, and their mixed oxides, $MO_{2\pm x}$, are solid solutions of oxygen defects (vacancies or interstitials) in a fluorite-type lattice. Noncongruent sublimation and, in the uranium-rich oxides, a marked increase in the sublimation rate at hyperstoichiometric compositions are the salient aspects of the high temperature behavior of these compounds, which in nuclear reactor applications may entail considerable technological drawbacks. This problem was thoroughly investigated in the past. Yet, while, from one side, a number of models have been developed, based on theoretical approaches of various complexity, experimental data remain scanty and imprecise at high temperatures, where classical thermodynamic measurements are difficult. Thus, most of the available experimental data on equilibrium vapor pressure pertain to the total pressure. Endeavors to analyze by mass spectrometry (MS) the equilibrium vapor in Knudsen-effusion experiments were only partially successful: in all cases, only the pressures of UO_2(g) and UO(g), the major vapor species in the hypostoichiometric range in the vicinity of O/U = 2.00, could be measured with an adequate precision, while the quantitative analysis of the other species led to less precise or even dubious results. For the hyperstoichiometric oxide, the situation is much worse, the data being there almost conjectural. There are different reasons for this failure, which are in part rooted in the nature of the examined compound and in part in the analytical method. The example of UO_2 is in fact paradigmatic.

(a) The sensitivity of the equilibrium partial pressures of the stoichiometrically noncongruent species (mainly of UO_3(g), UO(g) and U(g)) on the deviation from stoichiometry, *x*, of the condensed phase is very high. This fact, as well as the difficulty of adequately controlling the sample composition during vaporization experiments, makes the vapor analysis uncertain.

(b) Whenever polyatomic oxide molecules are analyzed, the problem is faced of interpreting the ionization and fragmentation processes occurring in the mass spectrometer. One molecule produces, for a given ionization process (e.g., electron collisions, photon interactions, or thermal excitation), a typical spectrum of ions, the so-called "signature", which depends on the ionization conditions. If these are kept constant, the analysis of the signature makes it possible to deduce the original concentration of the molecule in the gas mixture. The problem becomes more delicate if a mixture of original molecules is analyzed, in which the mass of some components corresponds to that of one of the fragments of larger molecules. In principle, the calculation of the molecular fractions from the measured ion densities is still possible, however, in practice, serious restrictions may arise, entailing dramatic losses of precision, which may invalidate any analytical approach. This difficulty is always encountered when a quantitative analysis of the UO_x vapor components is attempted.

In this work, ionization and dissociation of vapors of uranium and plutonium oxide were investigated with the aim of providing the necessary database for deducing the actual concentrations of the gaseous species MO_x in an effusing molecular beam from mass spectrometric measurements.

II. Experiment

Aim of the reported experiment was to obtain a set of mass spectrometric measurements of well characterized equilibrium vapor mixtures over UO_2 and PuO_2, and, hence (a) to work out and check for self-consistency the relevant set of ionization and fragmentation threshold energies for the main gas species in equilibrium with solid $UO_{2\pm x}$, from the trioxide to atomic uranium, and (b) to deduce a semiempirical formula, from which the original fractional compositions of the various species can be calculated from the MS signals.

The major experimental difficulty was to produce a stable molecular beam during a sufficiently long time to carry out a full set of measurements at different ionization energies up to 60 eV (the typical useful range in MS measurements). An effusion Knudsen cell was used to this purpose. Since, however, the MS detection efficiency of a molecular beam of a condensable species is much lower than for gaseous species with comparable ionization potentials, effusion rates were required, which can be produced only at high temperatures. For instance, in *hypostoichiometric* uranium dioxide, a sufficiently high UO partial pressure can only be obtained above 2200−2300 K. On the other side, in the more volatile *hyperstoichiometric* oxide, production of a stable molecular beam of UO_3 during measure-

10.1021/jp992405f CCC: $18.00
Published on Web 11/25/1999

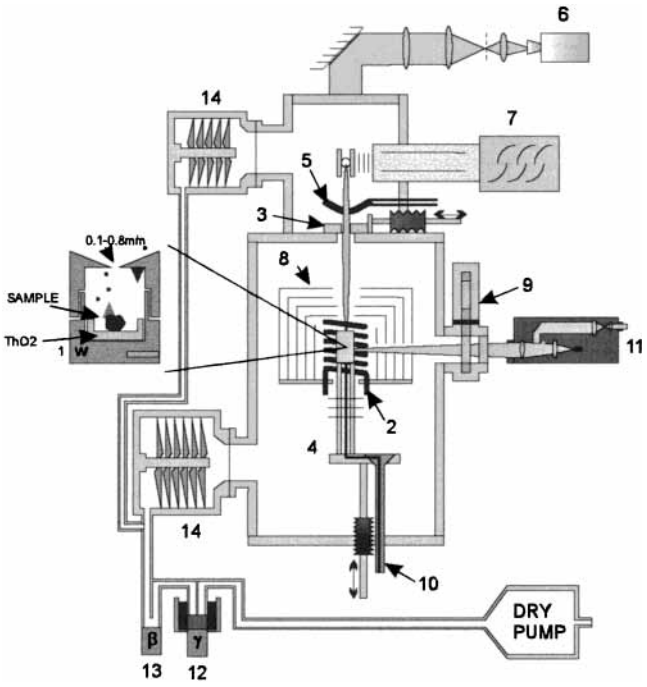

Figure 1. Scheme of the setup. Legend: (1) Knudsen cell whith black−body hole; (2) tungsten resistance coil; (3) chopper to stop the molecular beam (reference noise diagram); (4) facilities to lift cell for fast heating; (5) cold trap (LN) to reduce noise; (6) CCD camera to align the cell and chopper holes; (7) quadrupole mass spectrometer; (8) thermic shield (three tungsten and four tantalum shields); (9) revolving protection windows; (10) inlet gas capillar; (11) linear pyrometer; (12) γ counter with cold trap (LN); (13) β counter; (14) turbo molecular pump.

ment times of the order of 0.5 h requires an adequate control of a high oxygen potential in the effusion cell, entailing serious corrosion problems.

A. Setup. The setup used (Figure 1) consists of a water-cooled housing with a resistance furnace ($T_{max} = 3000$ K) surrounded by seven cylindrical thermal shields, closed at the top and the bottom. The Knudsen cell (20 mm height × 10 mm diameter) is placed on a special mounting, which can be lifted into the furnace when this has reached the desired temperature (this avoids useless residence of the sample in the furnace during the long heat-up and degassing stage). A flexible capillary connected at an ending small ceramic cylinder provides the cell with a gas inlet controlled by an electronically steered microvalve. Depending on the fixed oxygen potential, a cell of tungsten or thoria was used. At the top of the furnace, on the central axis, a circular aperture of approximately 10 mm diameter conveys the molecular beam effusing from the cell to the upper flask of the housing. This is placed at only ∼10 mm from the deck of the outermost thermal shield; it consists of a copper plate cooled by an independent circulating water loop. A second diaphragm, above this copper plate, mounted on a micrometric $x-y$ table, gives the beam the access to an upper chamber where the ion source of the mass spectrometer is mounted. This is a quadrupole (Balzers QMA400) with 90° entry angle.

The ions, separated according to their mass/charge ratio, are detected electrically either directly by a Faraday collector (FC) or through a secondary 17-stages electron multiplier (SEM). The first has a limit of about 10^{-16} A for measurement times of a few seconds. The SEM has a current gain of up to 10^8 and is very rapid and effective; it requires, however, a correction for mass discrimination. This is normally obtained by comparing spectra of standard specimens taken with SEM and with FC. In practice, though the SEM exhibits sufficiently stable amplification factors, checks were made at frequent intervals.

A large cold trap with circulating liquid nitrogen (LN) surrounds the ion source. A shutter, placed above the copper plate diaphragm, is opened only during the effective measurement time. The temperature is measured through a window protected by a revolving set of optical glasses. At the top of the instrument, a video camera, provided with a visible coaxial laser beam, is focused on the hole of the cell, to help aligning the effusing molecular beam with the entry hole of the ion source of the quadrupole. Two parallel turbomolecular pumps producing a final vacuum of less than 10^{-9} Torr evacuate the furnace vessel and the MS chamber. A third turbomolecular pump and a powerful oil-free Leybold Dryvac pump provide primary vacuum.

The entire setup, including the high-vacuum pumps, is installed in a large glovebox under purified nitrogen atmosphere.

Thanks to the good vacuum, and to the presence of the very effective LN trap, the rest-gas noise under the highest temperature (3000 K) effusion conditions (mainly due to hydrocarbons) could be reduced to ensure a measurement dynamic range of *not less* than 5 orders of magnitude.

B. Measurements. The experiments were carried out at temperatures between 1700 and 2500 K, on samples of various stoichiometries.

The oxygen partial pressure in the rest gas could be easily kept around the equilibrium values over the investigated *hypostoichiometric* oxides, so that stoichiometry control of these samples was not problematic.

For UO_{2+x} ($x \leq 0.15$), the equilibrium pressure assumes a sufficiently high value at 1700 K. At this temperature, $p(UO_3)$ is up to 4 orders of magnitude higher than $p(UO_2)$. To avoid reduction due to noncongruent evaporation, a relatively large oxygen partial pressure ($\Delta G(O_2) = -30$ kcal/mol) was produced in the cell with a buffer gas mixture of CO_2/CO. Under these conditions, though the heater and the thermal shields suffered marked corrosion during the experiment, the sample, contained in a thoria cell, exhibited a stable vaporization rate.

The measurements were normally started at the highest ionization energy; this was then gradually decreased by keeping the total electron beam current constant. This was controlled by adjusting the current (and hence the temperature) of the emission filament. This adjustment produces a variation of the energy spectrum of the electrons, since these are accelerated by a gun of relatively simple design. Altogether, electron emission, simple electron optics, and in addition, space charge effects produced a large offset between the applied cathodic voltage and the effective electron energy spectrum. This was, therefore, experimentally calibrated by taking the established first ionization potentials of silver, xenon, and krypton as standards, which cover an energy range from 7.5 to 24 eV. The test revealed that the offset is *not* constant but *increases* linearly with the applied cathodic voltage. The offset measurements are plotted in Figure 2. The straight line, defined by the *three* standard ionization energies, was used to check the appearance potential of a number of gaseous species, extrapolating the reference curve up to 35 eV. The results exhibit a sufficiently good linear dependence (regression coefficient $R = 0.998$) on the cathodic voltage for further extrapolating the scale-up to 60 eV. The 95% confidence band about the regression line is less than 0.1 eV over the interested interval.

In the calibration curve of Figure 2, both gases and condensable species are included. While mass spectrometer measurements of gaseous species are very accurate and reproducible

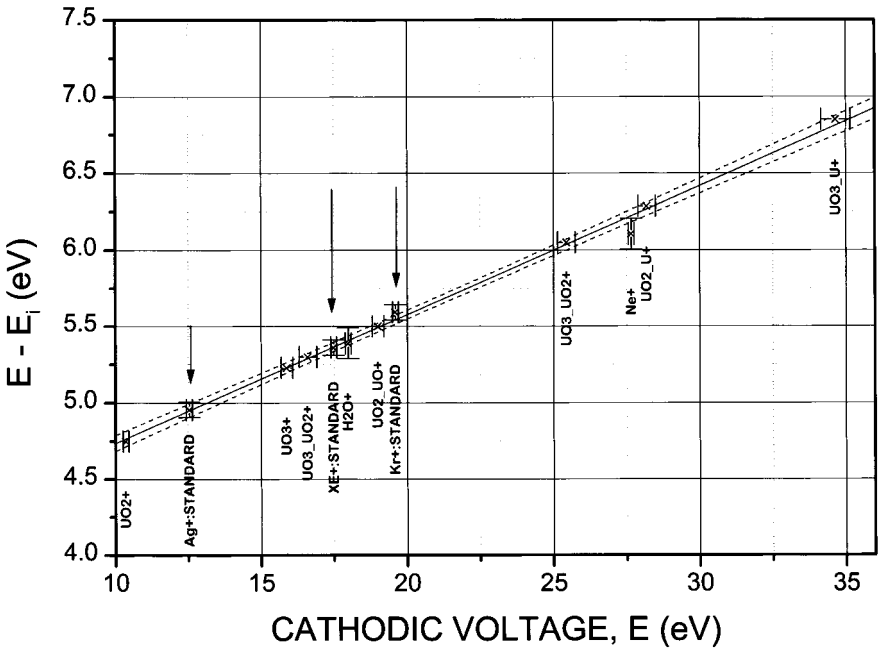

Figure 2. Offset of the ionization potential with respect to the applied cathodic tension in the MS electron gun. The arrows indicate the three standards used for defining the interpolating straight line. The dashed lines define the 95% confidence interval if all points are accounted for.

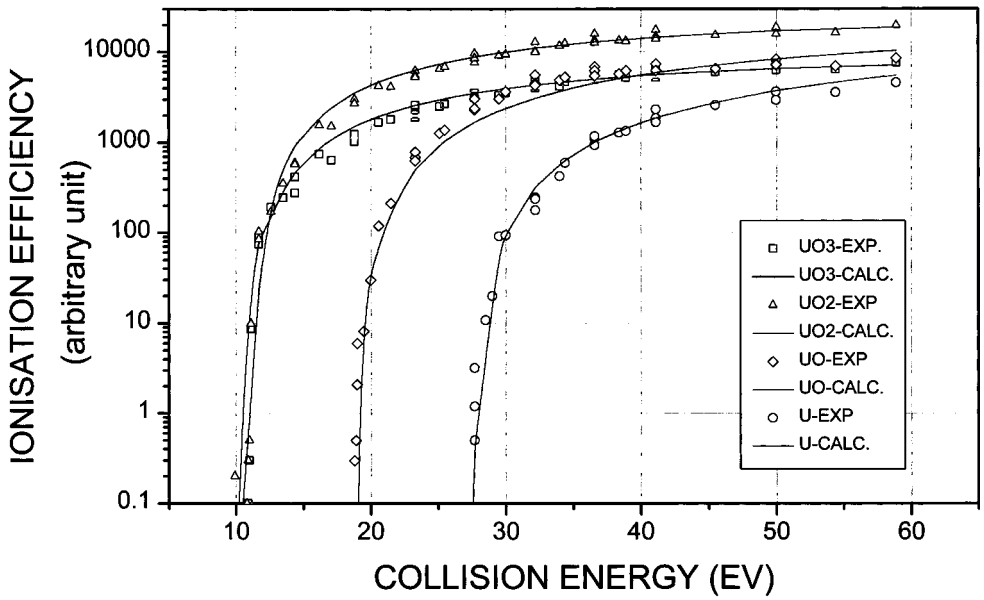

Figure 3. Measured ionization efficiency of the equilibrium vapors over $UO_{2.15}$ at 2200 K. UO_3(g) is the largely dominant species. In the plotted current range, UO_2^+, UO^+, and U^+ are only dissociation products of UO_3. The solid lines represent the prediction of eq 4.

over the explored range of energy, those based on ionization of condensable molecular beams are subjected to larger random fluctuations.[1] However, the determination of the appearance potential is sufficiently accurate also for these species; the error is indicated in the graph by the horizontal bar. As an example, measurements of the equilibrium vapors over $UO_{2.15}$ are plotted in Figure 3.

III. Analysis

The faced problem consists in expressing the MS ion current measurements, S_j, of the main vapor species of the vaporizing oxide in terms of general parameters, i.e.,

$$S_j = A[\sigma_j^o x_j + \sum_{k=1}^{N_j} \sigma_j^k(E) x_k] \qquad (1)$$

where x_j is the real concentration of the neutral species $\langle j \rangle$, σ_j^o is the first ionization cross section of $\langle j \rangle$ (the superscript "o" will be omitted hereafter) for producing an ion $\langle j^+ \rangle$, and σ_j^k is the probability that this latter is alternatively formed by ionization/fragmentation of a molecule $\langle k \rangle$. N_j is the number of possible mothers of $\langle j^+ \rangle$. A is a calibration constant of the mass spectrometer.

If the matrix of all cross sections, σ_j^k, at a given collision energy E is known, any set of MS measurements, S_j, can be converted into x_j by solving equation system 1. Therefore, providing once for all a general formula for $\sigma_j^k(E)$, expressed as a function of specific parameters for each species, pursues the solution of the general problem.

A. The Function $\sigma(E)$. Only highly simplified models can provide a usable expression for the ionization cross section at the impact energy, E. Even more problematic is the formulation

of the cross sections $\sigma_j^k(E)$, corresponding to the *dissociation* reactions of type "$e^- + \langle k\rangle \rightarrow \langle j^+\rangle + 2e^- +$ oxygen", which may result from a number of possible interactions of the incident electron with the quantum electronic states of the target molecule.

Some remarks on the inelastic scattering models are in order here, to justify the choice of an approximate expression for $\sigma(E)$.

a. Ionization of Heavy Atoms and Molecules. Let us start from Bethe's electron scattering model[2] obtained from Born's first approximation of the hydrogen atom. The ensuing simple expression for σ is rather transparent, being formally similar to that obtained by Bohr[3] using a classical (nonquantum mechanical) treatment,

$$\sigma = \frac{4\pi z^2 e^4 a_0}{v^2 m E_j}\ln\left(\frac{v^2 m}{2E_i}\right) \Rightarrow \frac{A}{EE_i}\langle r^2\rangle \ln\left(\frac{E}{E_j}\right) \qquad (2)$$

where v is the velocity of the incident electron, z is the charge number of the target atoms, and E_i an average electron energy loss per ionization event.[4] In the first right-hand-side term of eq 4, the argument of the logarithm defines a sharp threshold at $1/2mv^2 = E = E_i$, whose physical meaning is that the inverse of the collision pulse time must be *at least* equal to an appropriate average frequency of the electrons in the target atom corresponding to the energy E_i.[5]

A somewhat more accurate treatment provides an expression of σ in terms of the mean-square radius of the outer electron shell $\langle r^2\rangle$.

Despite the crudity of the original model, eq 2 is able to provide a coarse fit to experimental ionization curves of a number of heavy atoms and molecules. The parameter E_j is formally defined as an *effective* ionization potential. This definition is adequate if ionization currents are analyzed in the not-too-close vicinity of the appearance potential.[6] In fact, the experiment shows that, there, the dependence of σ on E is effectively linear. At higher energies above the threshold, the slope markedly decreases, until at approximately $E/E_i = 2.7$, where the curve of eq 2 presents a maximum. It was, however, very early recognized [7] that, compared to eq 2, the observed ion current vs energy shows in most cases a weaker dependence on E at energies just above the threshold, and the maximum is shifted with respect to that predicted by eq 2. The causes of this discrepancy, which reside both in the limits of the model and in the effective experimental ionization conditions, can be summarized as follows.

(1) Numerical calculations, based on more realistic models of the atomic structure of the target, lead to a less steep dependence of σ on E, the cross section increase being *not* expressed in terms of the threshold energy of a single, virtual transition at $E = E_j$, but rather by a sum of contributions of transitions with energies E_j^n, each one having a distinct weight function, g.

If the energy loss of the projectile during the collision is small compared with its initial energy, g is a nearly linear function of the modulus of the variation of the momentum of the incident electron and the simplified eq 2 is obtained. For larger electron energy losses, however, the dependence on K strongly deviates from linearity and eq 2 becomes less and less precise.

(2) In complex atoms, different low-lying ionization states can be reached. Some of them may be only slightly above the ion ground level, so that the ionization can take place along different paths with distinct relative probabilities. If even at low collision energies a significant fraction of ions is formed in excited states, the apparent ionization potential is higher than that referred to the ion ground state, and a negative compensation of the measured ionization potential may be necessary.

(3) Furthermore, if condensable target atoms are produced in a high-temperature source, some of them may have been excited into metastable states, whose half-life is long enough compared with the atom flight time. In this case, the measured ionization potential must be corrected for the positive energy shift of the initial state. Mann[8] gives an example of an approximate correction for thermal excitation of uranium; starting from the compiled levels of the uranium atom, he calculated the fractional population in metastable states, as well as the probability of the (four) main ionization paths. This correction term was estimated for the investigated molecules and applied to our data. For instance, at 2000 K, the resulting shift of the appearance potential, including that of point (2), is of the order of 0.1−0.2 eV.

(4) Since the electrons of the beam are emitted by a filament at temperature T, they are expected to exhibit a Maxwellian energy distribution. This has an influence on the apparent collision cross section, for which a correction can be estimated. Straightforward calculations lead to the approximated formula

$$\sigma(E \approx E_i) \cong \text{const}\frac{E - (E_i + 2RT)}{E_i} \qquad (3)$$

A finite cross section is therefore predicted down to energies *2RT* below the threshold energy. Furthermore, eq 3 predicts a constant shift (the order of 0.5 eV) of the zero of the appearance potentials in the energy scale. This correction is, therefore, automatically accounted for in the assessment of the effective energy scale reported in section II.B.

The effects described in points (1)−(4) can be regarded as perturbations affecting the relation between the empirical ion appearance potential and the defined ionization energy. The last to be examined is that caused by nonideal impact conditions in the ionization chamber (e.g., effective electron energy distribution, space charge disturbance, electrical field penetration, and boundary effects).

(5) As mentioned in section 2, when a cathodic voltage E^0 is applied in the MS ion source, electrons are produced which can collide with atoms with energies ranging from a distinct maximum to much lower values. Though, when E^0 is varied, the *total* electron current is maintained constant, one can expect that the *fraction* of electrons possessing a given energy E varies with E^0 according to a continuous function $f(E,E^0)$. Knowing this function would enable the average cross section for a threshold ionization energy E_i to be calculated as

$$\bar{\sigma} \div \int_{E_j}^{E} A\langle r_i^2\rangle \frac{\ln(E/E_i)}{EE_i} f(E)\, dE \equiv A\langle r_i^2\rangle \frac{\ln(\bar{E}/E_i)}{\bar{E}E_i}(\bar{E} - E_j)F(\bar{E}, E_j) \qquad (4)$$

where $\bar{E}$ is an effective energy, which is near to E. The introduction of the cumulative function $F(\bar{E})$ formally maintains in eq 4 a net truncation of the cross section at $\bar{E} = E_i$, implying identity between the *effective* ionization energy and the empirically observed appearance potential.

Endeavors were first made to evaluate eq 4 by assuming different expressions of the weight function $f(x)$, with the intent of providing a general criterion for evaluating $\bar{E}$ from the cathodic voltage E^0. For $f(x)$ corresponding to conjectural classical distributions, the agreement with the experiment was

generally mediocre.[9] In the absence of concrete arguments, we eventually simply defined $\bar{E}$ as the difference between the cathodic voltage and the corresponding offset plotted in Figure 2. This entails that eq 4 does *not* account for any "tail" of the cross section at energies below E_i.[10]

Having defined the effective energy, $\bar{E}$, enables F to be expanded in a Taylor series of powers of $\bar{E}$ and E_j:

$$\bar{\sigma}_i = A(\bar{E} - E_j)\sum_{n=0}^{\infty}\frac{1}{n!}(C_n\bar{E} + C_n^*E_j)^n\langle r_i^2\rangle\frac{\ln(\bar{E}/E_i)}{\bar{E}E_i} \qquad (5)$$

where C_n and C_n^* are constants. To this point, the question may be raised whether eq 5 still contains more physical information than any arbitrary spline function. In fact, a sufficiently precise fitting of eq 5 to the *whole set* of our experimental data is feasible by truncating the series just at the linear terms. The resulting dependence of F on the threshold energy is, therefore, very simple. For instance, all the measured ionization processes (i.e., including fragmentation) can be conveniently described by the cross section of eq 5, with only the *two* empirical coefficients of $\bar{E}$ and E_j (the constant term can be collected in factor A and taken equal to 1). We obtained

$$C_1 = -0.0153; \quad C^*_1 = 0.226 \qquad (6)$$

The simplicity of function F was of course not granted a priori; actually, it represents an experimental finding, which proves the suitability of eq 4.

b. Dissociative Ionization of MO_n Molecules. The above-mentioned considerations can also be applied to the ionization of the investigated oxide molecules. Though the electronic molecular structure of MO_n consists of a great number of complex states, the limits and the restrictions in the definition of the molecular ionization energy and the respective cross section are analogous to those encountered in heavy atoms.

Moreover, at a certain threshold collision energy, a molecule MO_n can undergo a vertical transition to an ionic state MO_n^+, with an excitation energy which can be large enough to produce a dissociation into $M^+ + nO$, whereby the fragments have a kinetic energy distribution very near to zero.[11] In more energetic collisions, the transition may lead to a repulsive state where the same fragments are produced with considerable kinetic energies. The definition of the ion appearance potential for these events is, therefore, more articulate than in the case of atomic ionization; depending on the extent of the Franck−Condon region of the ground state of the target molecule and on the state attained after electron collision, a sequence of appearance potentials, E_a, may be observed defined by

$$E_a(A) = E_{diss}(MO_n) + E_{ion}(M) + E_{exc}(M^+) + E_{kin}(M^+) + \sum E_{exc}(O) + \sum E_{kin}(O) \qquad (7)$$

where the symbols are self-explainatory.

A plethora of theoretical dissociation/ionization models have been attempted for simple molecules, but with mediocre success. The complexity of the situation in the case of the U−O system is well described in a paper by Fite et al.,[12] where the associative ionization collisions between uranium and oxygen are investigated at thermal energies. The situation is more complicated at higher collision energies, where additional chemi-ionization reactions are considered (e.g., rearrangement ionization, electron transfer).[13] In practice, even the most sophisticated chemielectron and photoelectron spectroscopic methods (see also refs 14−16) are unable to provide a complete picture of these complex ionization processes. Therefore, the published data on dissociation energies of MO_n have been up to now obtained from mass spectrometry measurements based on a simple analysis.

Finally, only the experiment can tell us how far does the first appearance potential of an ionic fragment fall with respect to the sum of the respective dissociation and ionization energies of the mother and how regular is the trend of the function $\sigma(E)$ at higher energies. In reality (see section III.A), the observed dissociative ionization cross sections for the oxides of uranium and plutonium up to 100 eV exhibit an energy dependence analogous to that of primary ionization. Furthermore, the observed thresholds effectively coincide, within the experimental error, with the sum of the corresponding chemical dissociation enthalpies and the ionization energies. On the basis of this observation, eq 5 is found to provide a sufficiently accurate description of the dissociation/ionization cross section as a function of the electron collision energy.

In conclusion, this function provides a general[17] expression of the matrix of the collision cross sections of the possible ionization events appearing in eq 1 and makes it possible to analyze the mass spectrometric signature of a given MO_n molecule. Hence, the initial purpose of providing a general solution method of eq 1 for any set of MS measurements at arbitrary collision energies is herewith accomplished.

The question remains, however, open, how the effective threshold energies used in eq 5 differ from the various rigorously defined ionization energies. Of the five points examined in the preceding sections, the energy shifts produced by the perturbations mentioned in points (4) and (5) have been automatically taken into account in the calibration of the energy scale. As for the effect discussed in point (1), the influence of the electronic configuration of the ground state of the molecule on the energy dependence of σ in the vicinity of the threshold may entail an intrinsic difficulty in the interpretation of E_j. Yet, the effective value of E_j appearing in eq 5 is clearly defined, and is not affected by these considerations.

Regarding points (2) and (3), the thermal excitation of molecules and ions at the temperatures of our experiments produces a shift of the apparent ionization potential. The published data on the ionization energies of uranium oxides obtained by mass spectrometry are not compensated for this effect, whose correction is expected to be smaller than the experimental error (see, e.g.. ref 18). In this work, the approximate calculations of the ionization energy shift in thermally excited U atoms[8] have been applied also to the UO and UO_2 molecules. To this purpose, we have used the calculated relativistic vertical ionization energies published by Allen et al.[19] The resulting thermal excitation correction of the ionization energy at 2500 K is, in both cases, below 0.1 eV. These corrections, which have little significance in the first ionization potentials of UO and UO_2, are probably also negligible in UO_3 ($E_i \approx 10.$ eV), whose electronic states are, however, unknown.

c. Electron Affinity. Among the molecules examined here, UO_3 has a very high electron affinity, $E_A = 5.2$ eV (a similar electron affinity was also measured in UF_6, a thoroughly investigated hexavalent uranium compound[20,21]). Molecules exhibiting a large electron affinity have a relatively large positive ionization potential compared to the dissociation energy. When the threshold energies of these two processes are too close, the probability that dissociation takes place instead of ionization can be large, depending on the configuration of the excitation states of the ion. In the case of UO_3, the measured ionization potential is only of a few tenths of an electronvolt lower than the dissociation potential. Consequently, the ionization cross

TABLE 1: Measured Formation Energies of Ions and Neutral and Positive Single-Charged Fragments

(a) UO_x

mother/daughter	$2\sqrt{\langle r^2\rangle}$ (au)	U^+	U	UO^+	UO	UO_2^+	UO_2	UO_3^+
UO_3	7.8	27.6 ± 0.3	21.6	19.3 ± 0.2	13.8	11.3 ± 0.2	5.9	10.8 ± 0.2
UO_2	7.2	21.7 ± 0.3	15.7	13.4 ± 0.2	7.9	5.4 ± 0.1		
UO	6.5	13.9 ± 0.2	7.8	5.6 ± 0.1				
U	5.5	6.1 ± 0.05						

(b) PuO_x

mother/daughter	$2\sqrt{\langle r^2\rangle}$ (au)	Pu^+	Pu	PuO^+	PuO	PuO_2^+
PuO_2	7.4	19.2 ± 0.3	13.1	12.8 ± 0.2	6.2	10.1 ± 0.1
PuO	6.6	13.0 ± 0.2	6.9	6.6 ± 0.1		
Pu	5.6	6.1 ± 0.05				

section is expected to be a small fraction of the capture cross section. We have therefore assumed that

$$\sigma_i(UO_3) = K\sigma_i^o(UO_3) \tag{8}$$

where σ_i^o is given by eq 5 and K is an empirical constant to be deduced from the experiment. This assumption was validated by several measurements carried out on gas mixtures containing UO_3 in different concentrations.

IV. Discussion

A. Uranium Oxide. Mass spectrometric measurements of stable and well-characterized molecular beams produced by Knudsen cell effusion at temperatures above 2200 K were analyzed to obtain a self-consistent set of parameters to be fed into eq 5. The results are collected in Table 1a and Figure 4, where for each neutral species the energies required to produce the various ionized or neutral fragments are given in electronvolts per target molecule. In Figure 4, the numbers printed in bold characters represent the measurements obtained in this work, while the others have been obtained as differences from the corresponding reactions. The data set is, therefore, self-consistent. The values are averages over different measurements; the errors range from ±0.1 eV for primary ionization to ±0.3 eV for dissociation/ionization processes. The values of the electronic shell radii are taken from refs 22−23.

a. U^+. The measured first ionization energy of U (6.15 ± 0.05 eV) is within 2% in agreement with the average worked out by Gurvich[24] from more precise determinations based on optical measurements (6.193 ± 0.002 eV).[25−27]

b. UO_2^+. The ionization potential of UO_2 (5.4 ± 0.1 eV) coincides with that, mostly recommended, of Rauh and Ackermann.[18] However, the appearance potential of UO_2^+ in MS measurements reported in the literature ranges from 4.3 ± 0.6 eV to 5.5 ± 0.04.[8,28−31] This shows that, depending on the analytical method adopted, the appearance potential can be very close, as in our case, or significantly lower than the ionization energy. The value of the ionization potential of UO_2 recommended in Gurvich's Tables[24] is 5.44 ± 0.25 eV, whereby the assessed accuracy is almost 2 orders of magnitude lower than for elemental uranium.

c. UO^+. The obtained first ionization energy of UO is 5.6 ± 0.1 eV, the same value found by Rauh and Ackermann. The same ionization energy is obtained by applying to the appearance potential of UO^+ measured by Mann the corrections for the excitation reported in sections III.A.a.2 and III.A.a.3.

d. UO_3^+. Our appearance potential of UO_3 (10.8 ± 0.2 eV) is between 11.1 eV reported by Pattoret et al.[28] and 10.6 eV by Rauh and Ackermann. The corrections of section III.A.a can only be roughly estimated for this molecule; the first ionization energy can be placed in the interval 10.7 ± 0.25 eV.

e. Ionic Fragments. The appearance potentials of the various ionic fragments measured in this work are reported in Table 1a. The same data are shown in Figure 4a. The threshold energies for dissociation of the *neutral molecules* are calculated from the appearance potentials of the respective ions produced as fragments (see the figures at the right-hand-side of Figure 4a). These latter are in good agreement with the thermodynamic values of the total atomization energies of the reactions $UO_m \rightarrow U + mO$, reported in Gurvich's tables.[24] This agreement is particularly significant, as it corroborates the existing data of the uranium oxides, which so far have been assigned, in the TPIS tables, the low-precision class "VI-F".[32] This is especially significant for UO_3, whose dissociation energy is more uncertain; we obtained $D(UO_3) = 21.6 \pm 0.3$ eV, compared to published data between 20.8 and 21.8 eV.[33] The same good agreement is found for the dissociation of UO (7.81 ± 0.1 eV), for which there exists only one direct measurement (7.7 eV) by De Maria et al.[34] (a slightly different value of $D(UO) = 7.5$ eV was recalculated by these authors from Chupka data[35]). Finally, the dissociation energy of UO at 2000 K calculated from the thermodynamic measurements of Ackermann and Thorn[36] varies between 7.7 and 8.2 eV.

f. The Yield Factor K. Finally, the attenuation factor, K, was measured for the first ionization cross section of UO_3; this was evaluated from several effusion experiments of largely hyperstoichiometric UO_{2+x}, obtaining as an average

$$K = 0.363 \pm 0.005 \tag{9}$$

This means that, *at any energy $E \lesssim 60$ eV*, only approximately 36% of the collisions with UO_3 molecules lead to a positive ion formation, while the rest results into a dissociation into *neutral* fragments. Some specialists, aware of the low ionization yield of UO_3 with respect to the other uranium oxides, suggested disparate, sometimes extremely low values of K. Spurious results were mainly due to the difficulty of producing a well-characterized vapor with stable UO_3 partial pressure. In our experiment, the value of this factor was checked in several noncongruent vaporization experiments, where UO_{2+x} samples were progressively reduced by sublimation of oxygen-rich vapor mixtures. The value of K reported above accounts sufficiently well for the measured composition of the ionic species.

The set of the measured ionization/fragmentation energies have been inserted, together with the value of factor K, in eq 5 to fit all the MS measurements performed on molecular beams of various compositions and different ionizing electron energies.

An example is shown in Figure 5, where the apparent composition of the uranium-bearing ionic species over $UO_{2.10}$

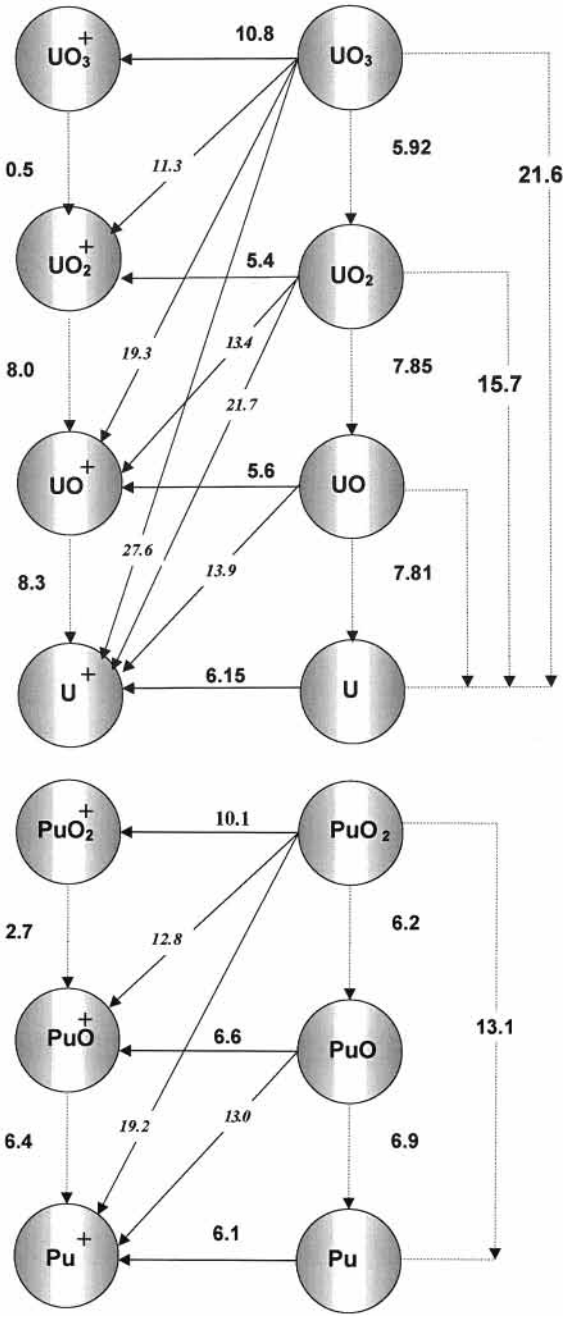

Figure 4. (a) Measured formation energies of neutral and positively charged uranium oxides. (b) Measured formation energies of neutral and positively charged plutonium oxides.

at 1700 K is plotted as a function of the ionizing electron energy. It can be seen that even at low ionization energies, a substantial correction is needed to obtain the right composition of the vapor from MS measurements.

B. Plutonium Oxide. The measured ionization potential of Pu^+ (6.10 ± 0.05 eV) agrees with the value recommended by Gurvich,[24] which is near to the most accurate optical measurements of Sugar[37,38] (this value is, however, up to 5% higher than those of other authors[39,40] and substantially differs from the oldest measurement of Berthelot (5.5 eV)[41]).

The results for plutonium oxide are collected in Table 1b and Figure 4b. For comparison, the only published data are those obtained from the Argonne National Laboratory;[42−45] our measured ionization energies of PuO_2 and PuO are higher, respectively, 10.1 ± 0.1 eV (instead of 9.3 ± 0.2 eV) and 6.6 ±0.1 eV (instead of 6.2 eV).[46] The ionization energy of PuO_2

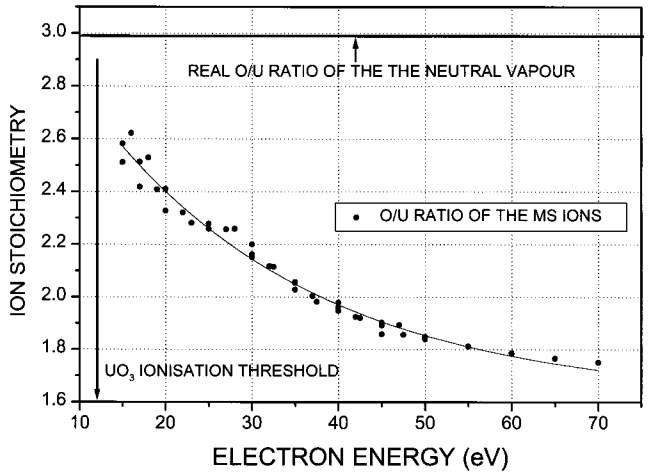

Figure 5. Composition of the ions in the equilibrium vapor over $UO_{2.10}$ at different ionization energies.

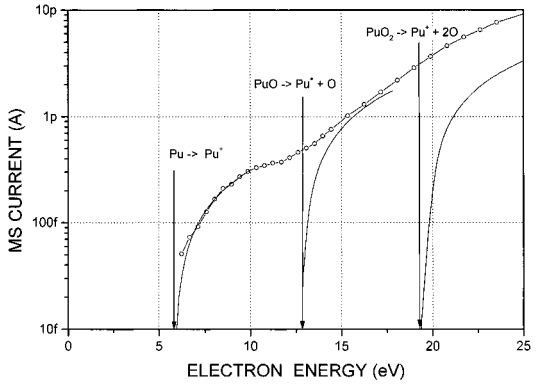

Figure 6. Ionization curve of Pu^+ as a function of electron energy of the equilibrium vapor over $PuO_{1.6}$. The major species here is PuO, whose dissociation produces a large amount of Pu^+ above 16.2 eV. The full lines represent the contributions from the primary ionization and from the two dissociation stages of PuO and PuO_2, respectively. In the ordinate scale the suffix "p" is for pico, and "f" for femto.

is near to that of UO_3. However, whereas the dissociation energy of UO_3^+ is only 0.5 eV, that of PuO_2^+ is 2.7 eV. This explains why, despite the large ionization energy, for PuO_2 we found a factor $K \cong 1$ (note that the electron affinity of PuO_2 is only 0.9 eV, against 5.2 eV of UO_3).

From the appearance potential of PuO^+ by dissociation of PuO_2 (12.8 eV), and of Pu^+ from PuO (13.0 eV), we deduce a dissociation energy for $PuO_2 \rightarrow PuO + O$ of 6.2 eV and for $PuO \rightarrow Pu + O$ of 6.9 eV; both values are very close to the recommended formation enthalpies (respectively, 6.24 and 6.85 eV). These data are corroborated by the measured appearance potential of Pu^+ fragments from PuO_2 dissociation (19.2 eV), which is in line with the latter. The precision of our data is of the order of 0.1 eV. The uncertainty due to the energy scale is of the order of 2%; this error, however, affects to a much lesser extent the dissociation energies obtained by difference. As an example, Figure 6 shows the MS measurements of Pu^+ effusing from a $PuO_{1.6}$ sample, at different ionization energies. The three stages, respectively, governed by ionization of atomic Pu(g), fragmentation of the monoxide (the major species in this case) and of the dioxide, are indicated by the curves in the figure.

Our results show that, contrary to uranium, atomic plutonium has lower ionization energy than the monoxide. In the above-mentioned reference, Rauh and Ackermann observed that monoxides are generally more easily ionized than the respective metal; in this context, however, calcium and hafnium represent

clear exceptions. Apparently, plutonium exhibits the same behavior as the latter elements. This is likely connected to the very strong f−p hybridization in the oxygen−plutonium bonding,[47] which is also responsible for to the observed high stability of PuO_2, whose saturated bonding entails a very large ionization energy (10 eV. compared to 5.4 eV of UO_2).

V. Conclusion

Two results were obtained in this work.

(i) First, a complete set of ionization/fragmentation energies of the uranium and plutonium oxides was obtained and compared with the existing thermodynamic data.

(ii) Second, it was found that these energies can be used as fitting parameters of a relatively simple function, which provides a general expression of the effective cross section of all the observed ionization and fragmentation processes at different electron collision energies. Particular examples are as follows.

(a) Though the cross section formula contains an empirical normalization function, it can be generally applied to calculate the number of ions and ionic fragments produced by electron collisions in the range up to ∼60 eV.

(b) With reference to the problem presented in the Introduction, we have finally shown that MS measurement of mixtures of MO_n gas molecules can be analyzed even in the presence of significant fragmentation processes. The accuracy of the resulting concentrations of the neutral species is not worse than that obtained by using reference gas mixtures (what is rarely possible).

References and Notes

(1) At equal effusion rates, gases have much higher ionization efficiency, on account of the fact that in the ionization chamber individual atoms may pass several times across the electron beam with different incidence velocities, whereas condensable molecules pass through only once.

(2) Bethe, H. *Ann. Physik* **1930**, *5*, 325.

(3) Bohr, N. *Philos. Mag.* **1913**, *24*, 10; **1915**, *30*, 581.

(4) The original theoretical treatment of inelastic scattering deals with the momentum or energy loss rate of the projectile. The macroscopic or total collision cross section is, by definition, inversely proportional to the average energy loss per collision event. For this reason, in the following approximated expressions of σ, the proportionality to $1/E_i$ is explicitly maintained.

(5) It is worth noting that if, after collision, the projectile is undeflected, the argument of the logarithm is multiplied by a factor of 4. Such a formula, referred as scattering cross section between heavy particles and electrons (see, e.g.: Fermi, E. *Nuclear Physics*; University of Chicago Press: Chicago, 1962; p 30), is sometimes taken as a theoretical description of the ionization cross section. This factor significantly reduces the slope of the logarithm function at low and moderately low energies. However, if the incident electron acquires in the collision a transversal momentum comparable to that given to the electron of the absorber, eq 2 is more correct.

(6) This means at values of E/E_i by a few percents above unit. At energies very close to the threshold, the cross section dependence on E becomes more complex.

(7) Tate J. T.; Smith, P. T. *Phys. Rev.* **1932**, *39*, 270.

(8) Mann, J. B. *Journ. Chem. Phys.* **1964**, *40* (6), 1632.

(9) For instance, by taking for $f(x)$ a Gaussian distribution centred on the effective energy $\bar{E}$ with a standard deviation s, the integral in eq 5 in the vicinity of E_i assumes the form $\exp(-\Delta E^2/2s^2)\sqrt{2/\pi}s + \Delta E[1 + erf(\Delta E/\sqrt{2}s)]/2E_0$, where $\Delta E = E - E_i \gtrsim 0$. This equation predicts an exponentially decaying tail for energies below the effective threshold.

(10) One should remember that the appearance potentials, E_0, of the standards have been empirically fixed, as customarily made, at the intercept of the linear extrapolation of $\sigma = \sigma(E)$ with the axis $\sigma = 0$, starting from energies a few tenths of an electronvolt higher than the threshold.

(11) One of the fragments in the dissociation may be negatively charged and the other positively charged or neutral. The former case is similar to the dissociation $AB \rightarrow A^+ + B$, involving a higher appearance potential. The latter, governed by electron capture, has a different collision energy dependency.

(12) Fite, W. L.; Lo, H. H.; Irving, P. *J. Chem. Phys* **1974**, *60*, 1236.

(13) Young, C. E.; Dehmer, P. M.; Cohen, R. B.; Pobo, L. G.; Wexler, S. *J. Chem. Phys.* **1976**, *64*, 306.

(14) Halle, J. C.; Lo, H. H.; Fite, W. L. *J. Chem. Phys.* **1980**, *73*, 5681.

(15) Dyke, J. M. A.; Ellis, M.; Fehér, M.; Morris, A. *Chem. Phys. Lett.* **1988**, *145*, 159.

(16) Baker, J.; Barnes, M.; Cockett, M. C. R.; Dyke, J. M.; Ellis, A. M.; Fehér, M.; Lee, E. P.; Morris, A.; Zamapour, H. *J. Electron. Spectrosc. Relat. Phenom.* **1990**, *51*, 487.

(17) Function $F(E)$ depends on the features of the ion source used. Yet, we have examined ionization curves produced in a time-of-flight mass spectrometer, where a more sophisticated electron gun was installed. The results were nevertheless similar to those obtained using a simpler Quadrupole source. In fact, the collision energy dispersion is likely to a great extent caused by space−charge effects, which depend principally on the electron current density.

(18) Rauh, E. G.; Ackermann, R. J. *J. Chem. Phys.* **1974**, *60*, 1396.

(19) Allen, G. C.; Baerends, E. J.; Vernooijs, P.; Dyke, J. M.; Ellis, A. M.; Fehér, M.; Morris, A. *J. Chem. Phys.* **1988**, *89* (9), 5363.

(20) Beauchamp, J. L. *J. Chem. Phys.* **1976**, *64*, 929.

(21) Compton, R. N. *J. Chem. Phys.* **1977**, *66*, 4478.

(22) AA. VV. *Construction of the Equation of State of UO_2 up to the Critical Point*; Project Report 930066; INTAS: Brussels, 1997.

(23) Mann, J. B. *J. Chem. Phys.* **1967**, *45*, 1646.

(24) Gurvich, L. V. *Termodinamiceskie svojstva individual'nych vescestv (Thermodynamic properties of individual substances)*; Nauka: Moscow, 1982; Tom IV, p 181 et sgg.

(25) Jones, G. S.; Itzkan, I.; Pike, C. T.; Levy, R. H.; Levin, L. *IEEE J. Quantum Electron.* 1976, *12*, 111.

(26) Solarz, R. W.; May, C. A.; Carlsen, L. R.; Worden, E. F.; Johnson, S. A.; Paisner, J. A.; Radziemski, L. J. *Phys. Rev. A* **1976**, *14*, 1129.

(27) Lias, S. G., et al. *J. Chem. Phys. Ref. Data* **1988**, 17 (Suppl. 1).

(28) Pattoret, A.; Drowart, J.; Smoes, S. In *Thermodynamics of Nuclear Materials*; IAEA: Vienna, 1968; p 613 et sgg.

(29) Blackburn, P. E.; Danielson, P. M. *J. Chem. Phys.* **1972**, *56*, 6156.

(30) Chupka, W. A. Report ANL 5786, Argonne National Laboratory: Illinois, 1957.

(31) Younes, C. L.; Nguyen, D.; Pattoret, A. *High Temp.-High Press.* **1981**, *13*, 105.

(32) Class F corresponds to uncertainties on the enthalpy of reaction between 0.1 and 0.3 eV.

(33) Ackermann, R. J.; Thorn, R. J. In *Thermodynamics*; IAEA: Vienna, 1966; Vol. I, p 254.

(34) De Maria, G.; Burns, R. P.; Drowart, J.; Inghram, M. G. *J. Chem. Phys.* **1960**, *32*, 1373.

(35) Chupka, W. A. Reports ANL 5753 (p 65) and 5786 (p 73); Argonne National Laboratory: Illinois, 1957.

(36) Ackermann, R. J.; Chandrasekhariah, M. S.; Rauh, E. G.; Thorn, R. J. Report ANL 7048; Argonne National Laboratory: Illinois, 1965.

(37) Sugar, J. *J. Chem. Phys.* **1973**, *59*, 788.

(38) Sugar, J. *J. Chem. Phys.* **1974**, *60*, 4103.

(39) Smith, D. H.; Hertel, G. R. *J. Chem. Phys.* **1969**, *51*, 3195.

(40) Belmonte, L.; Cavaliere, P.; Ferrante, G. *J. Chem. Phys.* **1974**, *61*, 3225.

(41) Berthelot, C. *J. Phys. Radium* **1962**, *23*, 447.

(42) Green, D. W. Report ANL-CEN-RSD 80-1; Argonne National Laboratory: Illinois, 1980.

(43) Blackburn, P. E.; Tevebough, A. D.; Bingle, J. D. Report ANL 7575; Argonne National Laboratory: Illinois, 1968.

(44) Blackburn, P. E.; Battles, J. E. Report ANL7445; Argonne National Laboratory: Illinois, 1968.

(45) Green, D. W.; Fink, J. K.; Leibowitz, L. Report ANL-CEN-RSD 82-1; Argonne National Laboratory: Illinois, 1982.

(46) The appearance potentials originally measured by Blackburn and Battles[44] were later corrected by Green[45] to obtain the ionization potentials. The applied correction procedure is, however, unknown.

(47) Gubanov, in a series of articles (see, e.g.: Gubanov, V. A.; Rosèn, A.; Ellis, D. E. *J. Phys. Chem. Solids* **1979**, *40*, 17), showed that in the actinide oxides f−p hybridization strength increases with atomic number and attains maxima in Np, Pu, and Cm.